Table I. Bond Strengths of Transition-Metal Compounds[a]

metal	IP[b]	PA[c]	M⁺-H	M⁺-O	M⁺-Me	M⁺-Cl	M⁺-F
Cr	6.77	193 ± 4	35 ± 4	77 ± 5	37 ± 7		
Mn	7.44	196 ± 3	53 ± 3	57 ± 3	>48		76 ± 12[d]
Fe	7.87	189 ± 5	58 ± 5	68 ± 3	68 ± 4	77 ± 12[d]	125 ± 12[d]
Co	7.86	184 ± 5	52 ± 4	65 ± 3	61 ± 4		
Ni	7.64	181 ± 2	43 ± 2	45 ± 4	48 ± 5		
Cu	7.73	150[l]	15[l]	33 ± 7[i]		>83[j]	95 ± 14[d]
Zn	9.39	154^{+7}_{-12}[e]	57^{+7}_{-12}[e]	33 ± 7[i]	68 ± 3,[f] 67.3 ± 1.0[k]	54 ± 6[g]	>59[e]
Ga	6.00			49 ± 12[d]			62 ± 12[d]
Cd	8.99	152 ± 20[h]	46 ± 7[h]	54 ± 3[d]	54.6 ± 1.0[k]		
Hg	10.44	126 ± 20[h]	53 ± 20[h]		69 ± 3,[d] 68.2 ± 1.0[k]	71 ± 7[d]	

[a] Reference 3c, unless otherwise stated; kcal/mol. [b] Ionization potential, eV, ref 11. [c] Proton affinity, DH(M-H⁺), kcal/mol. [d] From data in ref 13, 15. [e] This work. [f] Reference 20. [g] Reference 26. [h] Reference 19. [i] Reference 14; value is a lower limit, see text. [j] Jones, R. W.; Staley, R. H. *J. Am. Chem. Soc.* 1980, *102*, 3794. [k] Reference 28. [l] Predicted from data in ref 3c.

with doublet O^+, 77 kcal/mol up from the ground quartet state.[15] If this is taken as an upper limit, then $DH(Zn-O^+) \geq 117$ kcal/mol and $DH(Zn^+-O) \geq 19$ kcal/mol. The only instance in this work where ion transfer to Zn^0 was observed is for H^+ from the various protonated bases; the "closed-shell" nature of the transferred ion precludes multiplicity problems in this reaction.

Periodic Trends. Certain other thermochemical data are available from the literature and are compiled in Table I. These include data from ion-beam experiments, appearance and photoionization potentials, and ion/molecule reactions. Across the row, a general decrease in PA(M) is observed, with Zn having a lower PA than the first-row transition metals. Unfortunately, the only data for the neighboring elements Cu and Ga are the estimate for PA(Cu) based on promotion energy[3c] and the fact that GaH^+ does not appear to have been observed. It is noteworthy regarding the latter species that unless PA(Ga) is greater than 175 kcal/mol (considerably larger than for Zn), then $DH(Ga^+-H)$ will be negative and GaH^+ therefore unstable with respect to dissociation. The relatively strong Zn^+-H bond is consistent with Zn^+ being an s^1 configuration.[3c] The Zn^+-F bond strength of >59 kcal/mol derived here can be regarded as a relatively low bound; $DH(Cu^+-F) = 95 \pm 14$ kcal/mol[15], and on the basis of the promotion energy argument of Beauchamp and co-workers,[3c] it should be weaker than Zn^+-F. These halide bonds are considerably more polar than the M^+-H and M^+-CH_3 bonds discussed in ref 28, but for Cu vs. Zn, the electronegativity difference reinforces the bond strength ordering. The Ga^+-F bond strength of 62 ± 12 kcal/mol[15] is weak for a metal-fluoride bond, but the bonding may involve p orbitals, so that the promotion-energy correlation[3c] is not applicable. The chloride vs. fluoride bond strengths for Zn^+ parallel the general order $DH(M^+-Cl) < DH(M^+-F)$ observed for the first-row transition metals.[15] For the 2B elements Zn, Cd, and Hg, the uncertainties in the M^+-H bond strengths are large, but the order $Cd^+-H < Zn^+-H < Hg^+-H$[28] can be taken to be a mixture of electronegativity change and the lanthanide contraction. This order is not reflected in the neutral ordering Zn-H > Cd-H > Hg-H, where the unpaired antibonding electron affects the stability.[19] Similarly, the groups capable of sharing one electron in a bond, such as H· and Cl·, have neutral Zn-X bonds[19] weaker than their ionic counterparts, while oxygen, requiring a two-electron donation from the metal, has stronger neutral bonds, compared to the ionic analogues, for the 2B elements. On the basis of periodic trends, we predict that $DH(Zn^+-O)$ should be ca. 30 kcal/mol.

Conclusions

Zinc atoms and ions are relatively unreactive, in terms of atom abstraction or oxidative insertion, compared to the first-row transition metals, in spite of Zn^+ having the strongest metal ion to one-electron-donor ligand bond strengths of the first long series. This is a reflection of the filled-d-shell nature of Zn and Zn^+, with the bonding being primarily due to the s electrons.

Acknowledgment. We thank Prof. Ken Caulton for helpful discussions.

Registry No. Zn, 7440-66-6; Zn^+, 15176-26-8; ZnH^+, 41336-21-4; CH_5^+, 15135-49-6; N_2O, 10024-97-2; ZnO^+, 60131-08-0; CH_4, 74-82-8; N_2OH^+, 76412-54-9; CO, 630-08-0; HCO^+, 17030-74-9; NF_3, 7783-54-2; ZnF^+, 19624-01-2; HNF_3^+, 64709-84-8; $(CF_3)_2CO$, 684-16-2; $(CF_3)_2COH^+$, 79999-78-3; F_2, 7782-41-4; S, 7704-34-9; Cl_2, 7782-50-5; O_2, 7782-44-7.

(28) DiStefano, G.; Dibeler, V. H. *Int. J. Mass Spectrom. Ion Phys.* **1970**, *4*, 59.

Contribution from the Institut für anorganische Chemie, Universität Bern, CH-3000 Bern 9, Switzerland

Vanadium(II) Pair Excitations in $CsMg_{1-x}V_xCl_3$

HANS RIESEN and HANS U. GÜDEL*

Received August 9, 1983

Mixed crystals $CsMg_{1-x}V_xCl_3$ with x between 1% and 15% were prepared by the Bridgman technique. Single and double excitations to the ^2E, $^2T_1$, and $^2T_2$ states of $V_2Cl_9^{5-}$ dimers were studied by optical absorption and Zeeman spectroscopy. The ground-state exchange parameter is $2J = -187 \pm 5$ cm^{-1}. From an analysis of singly excited ^2E pair states the following orbital exchange parameters were derived: $2J_{a_1a_1} = -570$ cm^{-1}, $2J_{ee} = -195$ cm^{-1}. $J_{a_1a_1}$ is the dominant antiferromagnetic pathway as expected on the basis of overlap arguments.

1. Introduction

The exchange in the quasi-one-dimensional (1D) antiferromagnets $CsVX_3$ (X = Cl, Br, I) is unusually strong. Intrachain $2J$ values estimated from high-temperature magnetic susceptibility data are −160, −110 to −120, and −75 to −95 cm^{-1}, respectively.[1] The coupling constants between the chains

0020-1669/84/1323-1880$01.50/0

are also antiferromagnetic, but 4–2 orders of magnitude smaller than $2J$ in the sequence chloride, bromide, iodide.[2] This very pronounced anisotropy is a nice example of a magnetostructural correlation. $CsVX_3$ crystallize in the same hexagonal space group, $P6_3/mmc$, as $CsMgX_3$.[3,4] Mixed crystals $CsMg_{1-x}V_xX_3$ can be made, and with a suitable choice of x in the range 1–20% it should be possible to prepare samples with a sizable concentration of $V_2Cl_9^{5-}$ pairs. Optical excitations of these pairs contain information about exchange splittings in the ground and excited states, which, in turn, can be used to determine the principal orbital contributions to the net exchange coupling. In addition the mechanisms of electronic transitions in exchange-coupled systems can be conveniently explored in the pair spectra. In this sense the dimers obtained in the diluted crystals serve as useful molecular models for the concentrated pure antiferromagnets, which can only be treated theoretically by introducing a number of quite severe approximations.[2,5] The $V_2Cl_9^{5-}$ dimers in $CsMg_{1-x}V_xCl_3$ have D_{3h} point symmetry, and as a result of the 1D chain structure all the pairs are parallel, and their threefold axis coincides with the crystal c axis. For spectroscopic purposes this is a big advantage since it allows the measurement of polarized absorptions with respect to the dimer axis.

2. Experimental Section

The following starting materials were used for the synthesis of $CsMg_{1-x}V_xCl_3$: $MgCl_2$ (Great Western Inorganics 4N), CsCl (Merck Suprapur), $CsVCl_3$ (prepared according to ref 6). $MgCl_2$ was dried by heating to 400 °C under vacuum for 1 week and then purified by sublimation at 550 °C/30 °C under vacuum. CsCl was dried at 300 °C. Stoichiometric amounts of $MgCl_2$ and CsCl were then heated to 700 °C for 12 h in a silica ampule to produce $CsMgCl_3$. Single crystals of $CsMg_{1-x}V_xCl_3$ were obtained with the Bridgman technique, with the furnace temperature at 1100 °C and a pulling rate of 0.01 mm/min. All the products were characterized by powder X-ray diffraction, and the vanadium content was determined by atomic absorption spectroscopy.

Polarized single-crystal absorption spectra were recorded on a Cary 17 spectrophotometer equipped with a pair of Glan-Taylor prisms. The samples were cooled in a closed-cycle helium cryostat (Air Products CSA-202G). Due to the easy cleavage of the crystals parallel to the c axis spectra were recorded with the light propagating perpendicular to c. The electric vector could thus be chosen parallel (π) and perpendicular (σ) to the c axis.

Zeeman absorption experiments on sharp lines were performed as follows: The light of a 150-W halogen lamp was dispersed by a $^3/_4$-m monochromator (Spex 1702). A superconducting cryomagnet (Oxford Instruments, SM4) was used to cool the crystal down to 1.5 K and produce magnetic fields up to 5 T. The light passing through the crystal was detected by a cooled RCA 31034 photomultiplier using a chopper and a lock-in amplifier (PAR 186A).

3. Results

The low-temperature optical absorption spectra of single crystals of $CsMg_{1-x}V_xCl_3$ with $x = 1\%$ and 11% are compared with the spectrum of pure $CsVCl_3$[6] in Figure 1. The three spin-allowed transitions to $^4T_2$, $^4T_1{}^a$, and $^4T_1{}^b$ appear to be practically independent of concentration. They are therefore not a useful source of information for exchange effects. The spin-forbidden bands, in contrast, are strongly affected by the exchange coupling. Their overall intensity increases with

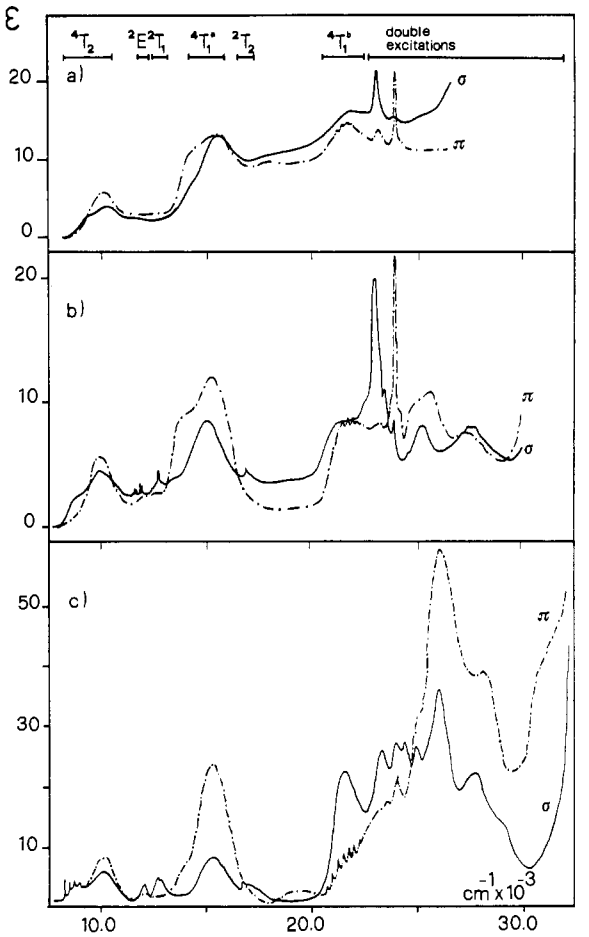

Figure 1. Polarized low-temperature absorption spectra of $CsMg_{1-x}V_xCl_3$: (a) $x = 1\%$, $T = 8$ K; (b) $x = 11\%$, $T = 12$ K; (c) $x = 100\%$, $T = 8$ K.[5]

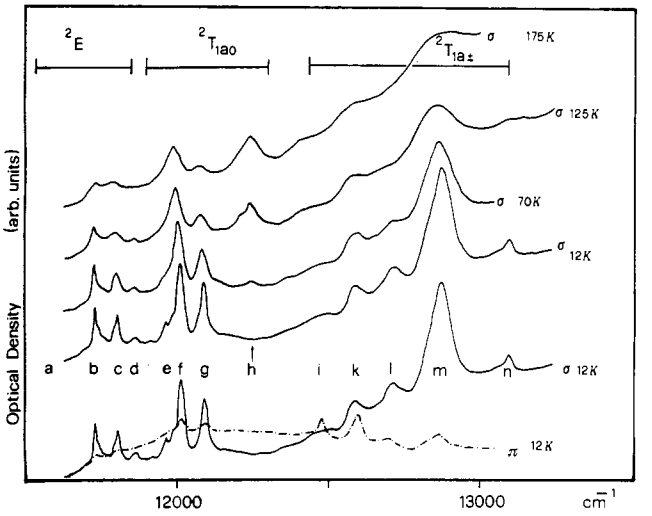

Figure 2. Polarized low-temperature absorption spectra of an $x = 10\%$ crystal and temperature dependence of the σ spectrum in the region of ^2E, $^2T_1$ single excitations.

increasing concentration. In the $x = 1\%$ crystal, in which more than 95% of all the vanadium(II) ions occur as single centers, the ^2E, $^2T_1$, $^2T_2$ single excitations are barely visible. But even in this very diluted crystal there are two sharp and relatively intense absorptions at an energy that corresponds to the sum of two spin-forbidden single excitations. These so-called double excitations are due to a very small number of vanadium pairs (less than 1% of all the vanadium ions) and, consequently, have very high oscillator strengths. This is also seen in the spectra of the $x = 11\%$ and 100% spectra, in which the high-energy

(1) Niel, M.; Cros, C.; Pouchard, M.; Chaminade, J. P. *J. Solid State Chem.* **1977**, *20*, 1.
(2) Hauser, A.; Güdel, H. U. *J. Magn. Magn. Mater.* **1983**, *31–34*, 1239.
(3) Niel, M.; Cros, C.; Vlasse, M.; Pouchard, M.; Hagenmuller, P. *Mater. Res. Bull.* **1976**, *11*, 827.
(4) McPherson, G. L.; Kistenmacher, T. J.; Stucky, G. D. *J. Chem. Phys.* **1970**, *52*, 815.
(5) Hauser, A.; Güdel, H. U. *Chem. Phys. Lett.* **1981**, *81*, 72.
(6) Hauser, A.; Güdel, H. U., to be submitted for publication.

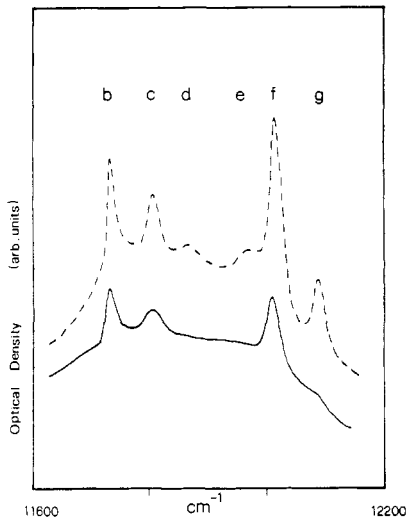

Figure 3. Concentration dependence of low-energy absorption bands in σ polarization: (—) 1.4 mol %, (- - -) 8 mol %. T = 12 K.

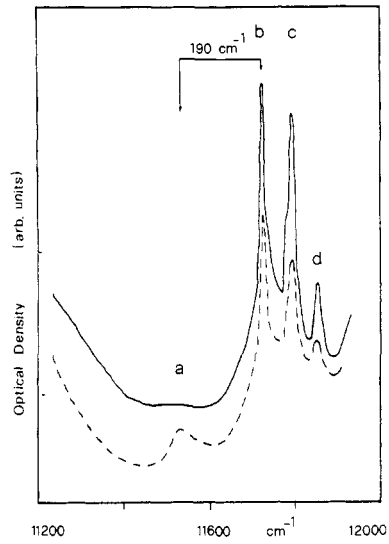

Figure 4. Single ^2E pair excitations at 12 K (—) and 80 K (- - -) in the σ spectrum. The bands are almost purely σ polarized.

part is dominated by double excitations. In the pure material they are more intense than the nominally spin-allowed bands.

The ^2E, $^2T_1$, and $^2T_2$ single excitations can be easily identified in the spectrum of the x = 11% crystal. They are sharp and show a great deal of fine structure, and in addition, they are all predominantly σ polarized. The region of ^2E and $^2T_1$ transitions is reproduced in Figure 2. The bands b, c, and d are considerably sharper than the higher energy bands f–n in Figure 2. We assign the former to ^2E transitions and the latter to $^2T_1$ transitions. In the following our emphasis will be on the ^2E transitions. Due to their sharpness they allow a more elaborate and detailed spectroscopic analysis. In addition, the theoretical treatment of ^2E pair transitions is well established, whereas the procedure for $^2T_1$ transitions is more doubtful due to the orbital degeneracy.

The bands b, c, and f have the same concentration dependence (Figure 3). They can therefore be assigned to the same chromophore. On the basis of the observed temperature dependences (Figure 2) they are attributed to $V_2Cl_9^{5-}$ dimers. The bands d, e, and g, on the other hand, have a distinctly different concentration behavior. They must be due to a higher cluster, most likely a trimer. Figure 4 shows the low-energy region of the ^2E dimer spectrum as a function of temperature. The hot band a appears 190 cm^{-1} below the cold band b. This hot band is part of the ^2E pair spectrum. It corresponds to

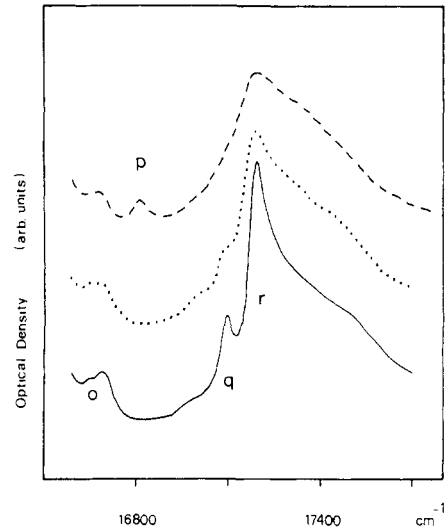

Figure 5. Temperature dependence of the σ spectrum in the region of $^2T_2$ excitations at 12 K (—), 54 K (···), and 90 K (- - -).

Table I. Positions (cm^{-1}), Half-Widths (cm^{-1}), Polarizations, and Extinction Coefficients (per Mole of Total Vanadium) of Absorption Bands in the Region of ^2E, $^2T_1$, $^2T_2$ Single Excitations in an x = 10% Crystal

band	position	half-width	polarizn	T, K	ϵ
a	11 538	30	σ	80	0.05
b	11 730	5	σ	12	0.5
c	11 804	5–10	σ	12	0.4
d	11 863	10–20	σ	12	0.07
e	11 973	10–20	σ	12	0.2
f	12 010	25	σ	12	1.0
g	12 089	25	σ	12	0.8
h	12 214	40	σ	127	0.2
	12 241	40	σ	127	0.3
i	12 478	30	π	12	0.3
k	12 575	40	σ	12	0.1
	12 602	30	π	12	0.3
l	12 710	40	σ	12	0.1
m	12 833	50	σ	12	0.7
	12 886	50	σ	12	0.1
n	13 087	25	σ	12	0.1
o	16 662	30	σ	12	0.1
	16 709	30	σ	12	0.05
p	16 822	40	σ	90	0.05
q	17 110	35	σ	12	0.15
r	17 206	40–50	σ	12	0.5

a transition originating in the triplet pair ground level, and the energy difference of 190 cm^{-1} is the singlet–triplet separation in the ground state. Another hot band, h, appears at 12 241 cm^{-1} (Figure 3). It is most likely a $^2T_1$ pair band. The absorption bands in the $^2T_2$ region have widths that are similar to those of the $^2T_1$ bands. Their temperature dependence is shown in Figure 5. Also in this region the hot band p can be clearly identified. The positions, half-widths, polarizations, and extinction coefficients of all the absorption bands of an x = 10% crystal in the ^2E, $^2T_1$, and $^2T_2$ region are collected in Table I.

The results of Zeeman absorption measurements on bands b and c are reproduced in Figure 6. Both band b and band c consist of more than one component in zero field. The principal component has the lowest energy in band b and the highest energy in band c. Band b clearly shows a Zeeman splitting in a field of 5 T parallel to c, even though the components are not individually resolved. In band c, on the other hand, the high-intensity component is unaffected by the magnetic field, whereas the weaker shoulder is split. Except for bands b and c the absorption bands are too broad for Zeeman experiments.

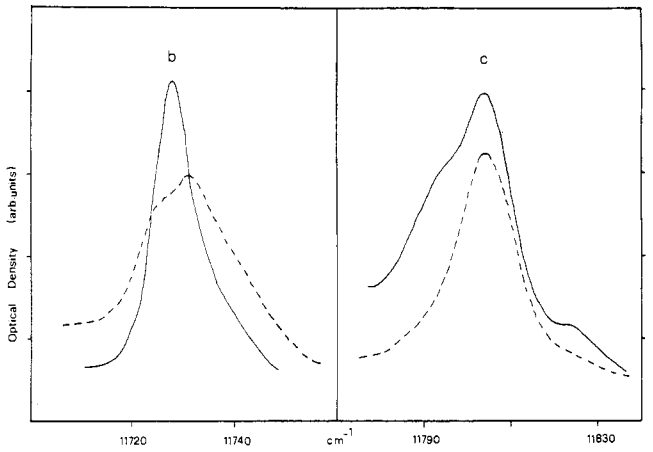

Figure 6. 1.4 K absorption spectra (σ polarization) of the bands b (left) and c (right) without (—) and with (- - -) a magnetic field of 5 T parallel to *c*.

4. Discussion

1. Dimer Ground State. The electronic ground state of vanadium(II) in octahedral coordination is $^4A_2$. In very diluted $CsMg_{1-x}V_xCl_3$ crystals the following ground-state parameters were determined by EPR: zero-field splitting 0.096 cm^{-1}, $g_\parallel = 1.973$, $g_\perp = 1.975$.[4] The exchange coupling in the dimer should therefore be well described by a Heisenberg type Hamiltonian:

$$H_g = -2J\mathbf{S}_a\cdot\mathbf{S}_b \qquad (1)$$

With $S_a = S_b = {}^3/_2$ and D_{3h} pair symmetry the pair levels of the ground state are characterized by $^1A_1'$, $^3A_2''$, $^5A_1'$, and $^7A_2''$. For antiferromagnetic coupling the singlet level has the lowest energy. The singlet–triplet separation is $-2J$. The high-energy quintet and septet levels are neglected in the following. The energy difference between singlet and triplet pair levels and thus the exchange parameter $2J$ can be directly determined experimentally from the energy difference between the two bands a and b in Figure 4: $2J = -190$ cm^{-1}. This rather elegant method of determining an exchange parameter is possible because both transitions a and b involve the same excited pair level. Information about the singlet–triplet separation is also contained in the temperature dependence of intensity of the various pair bands. All the bands observed at 12 K or below are cold bands originating in the $S = 0$ ground level. The hot bands, on the other hand, correspond to triplet transitions. The intensities of several cold and hot bands, which are isolated in the spectrum, are plotted vs. temperature in Figure 7. From a least-squares fit of the singlet and triplet Boltzmann population factors an energy difference of 180 cm^{-1} is obtained. This is in good agreement with the value determined above. Giving appropriate weight to the two methods of determination, we obtain $2J = -187 \pm 5$ cm^{-1}. This value can be compared with the value of -160 cm^{-1} estimated from the magnetic susceptibility of pure $CsVCl_3$ by a high-temperature series expansion approximation.[1] The exchange constants in a vanadium dimer and in the pure 1D antiferromagnet need not necessarily be the same. But we feel that the difference between the two numbers is at least partly due to the approximate character of the magnetochemical estimate, and the value of -187 cm^{-1} may be close to that in the pure material.

2. Singly Excited ^2E Pair States. Exchange interactions in the singly excited ^2E pair states are appropriately described by the Hamiltonian[7]

$$H_e = -2\sum_{ij} J_{ai\,bj}(\mathbf{s}_{ai}\cdot\mathbf{s}_{bj}) \qquad (2)$$

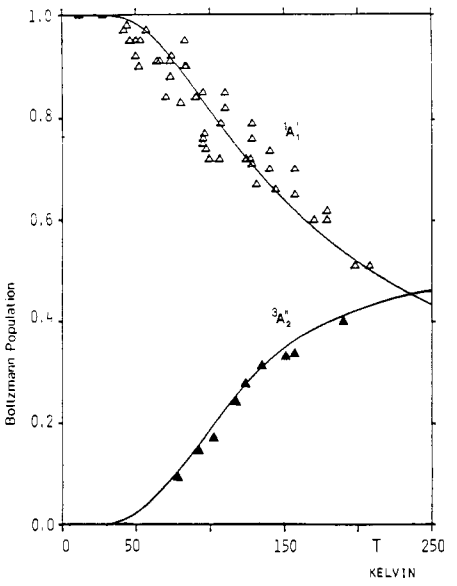

Figure 7. Experimental temperature dependence of intensity of the pair bands b, c, f, and m and the double excitation at 24 630 cm^{-1} (△) and the hot band h (▲). The solid lines are the result of a least-squares fit of the $^1A_1'$ and $^3A_2''$ Boltzmann populations to the observed intensities. They correspond to an exchange parameter $2J = -180$ cm^{-1}.

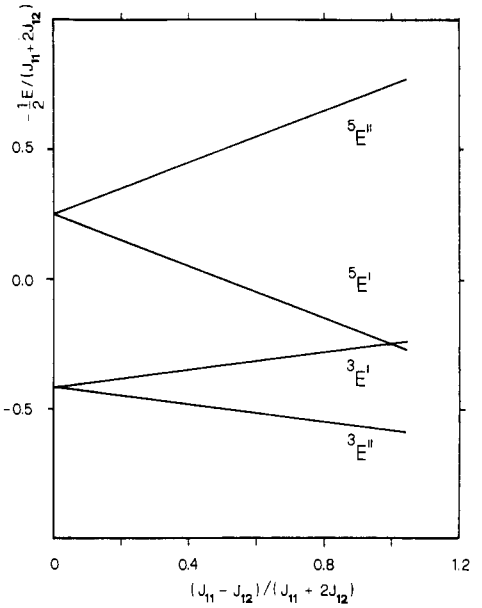

Figure 8. Exchange splitting of the singly excited ^2E state. Spin–orbit coupling and trigonal crystal field are neglected. The pair states are designated according to D_{3h} pair symmetry.

where i and j designate the singly occupied t_2 orbitals. A detailed theoretical analysis of singly excited ^2E states in a chromium(III) dimer of D_{3h} symmetry has been given by Dubicki and Tanabe.[8] We are using their notation and results. The one-electron orbitals

$$\xi = yz = 1 \qquad \eta = zx = 2 \qquad \zeta = xy = 3 \qquad (3)$$

are defined in the cubic coordinate frame of the single vanadium ions. There are only two independent parameters in D_{3h} dimer symmetry:

$$J_{11} = J_{22} = J_{33} \qquad J_{12} = J_{21} = J_{13} = J_{31} = J_{23} = J_{32} \qquad (4)$$

Under the action of the operator (2) and with neglect of

(7) van der Ziel, J. P. *Phys. Rev. B: Solid State* **1974**, *9*, 2846.

(8) Dubicki, L.; Tanabe, Y. *Mol. Phys.* **1977**, *34*, 1531.

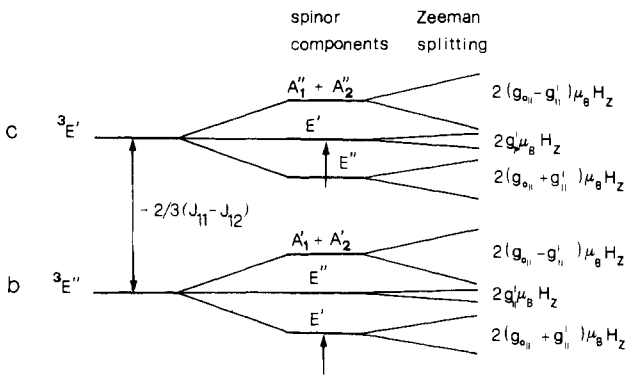

Figure 9. Splitting of $^3E''$ and $^3E'$ singly excited ^2E pair states as a result of spin–orbit coupling and trigonal crystal field. The allowed transitions to the E′ spinor components are indicated. The effects of an external magnetic field parallel to *c* are shown on the right-hand side. $g_{0\parallel}$ and $g_\parallel'$ are defined in ref 8.

spin–orbit coupling and trigonal crystal field effects, ^2E splits into the four pair states $^3E'$, $^3E''$, $^5E'$, and $^5E''$. This is shown schematically in Figure 8. Spin–orbit coupling and the trigonal crystal field in combination will lead to a further splitting of these excited pair states (Figure 9). From a comparison with known ^2E splittings in trigonal chromium(III) complexes we expect these splittings in the $V_2Cl_9^{5-}$ dimer to be on the order of 20–40 cm^{-1}.[9] The Zeeman splitting, which is also included in Figure 9, was calculated in ref 8 for the analogous $Cr_2Br_9^{3-}$ dimer. Relevant for our discussion is the expectation that in the $^3E''$ state the E′ spinor component has a large first-order Zeeman splitting, whereas in $^3E'$ the E′ component is only split by the orbital contribution.

Intensity of spin-forbidden (in the single ion) transitions in a dimer can arise either through a single-ion mechanism involving spin–orbit coupling or an exchange mechanism.[8] The selection rule $\Delta S = 0$ and the symmetry selection rules derived from the transformation properties of the dimer states apply for the exchange mechanism. This means that in our $V_2Cl_9^{5-}$ dimer only one hot band corresponding to the $^3A_2'' \rightarrow {}^3E''$ transition is allowed by this mechanism. All the absorptions observed in the low-temperature spectra obtain their intensity by a single-ion mechanism. Both the $^1A_1' \rightarrow {}^3E''$ and the $^1A_1' \rightarrow {}^3E'$ transitions have allowed components. This is shown in Figure 9. The E′ spinor components are spectroscopically accessible. The splitting is such that E′ lies below E″ in $^3E''$; in $^3E'$ the order is opposite.

On this basis and that of the observed band shapes, we assign the absorption bands b and c to the $^3E''$ and $^3E'$ transitions, respectively. In both bands the component with the highest intensity corresponds to the E′ spinor component. The E″ components are observed as weaker shoulders. They are not allowed with a single-ion mechanism but can possibly gain some intensity if the fiction of a purely isotropic exchange coupling is given up. Experience shows that deviations from the theoretically expected selection rules occur much more easily than deviations of energetic splitting patterns. Our assignment is fully supported by the results of the Zeeman experiments. As shown in Figure 9, we expect the principal component of band b to split in a magnetic field parallel to *c* into two components separated by $2(g_{0\parallel} + g_\parallel')H_z \cdot \mu_B$, while the splitting of the higher energy shoulder should be smaller than the bandwidth. For band c the situation is expected to be reversed: the shoulder should split and the principal component remain unaffected. This is in exact correspondence with the observed behavior. Assuming $g_{0\parallel} = g = 1.97$,[4] we determine $g_\parallel'$ from the observed Zeeman splitting: $g_\parallel' = -0.35$. This is in poor agreement with the $g_\parallel'$ value of −2.0 expected from first-order perturbation theory. It demonstrates that the first-order treatment is not adequate for large trigonal fields.

Having assigned the bands b and c to the $^1A_1' \rightarrow {}^3E''$ and $^3E'$ transitions, respectively, it is straightforward to assign the hot band a to $^3A_2'' \rightarrow {}^3E''$, the only allowed transition by an exchange intensity mechanism in this spectral region. It is expected to be σ polarized and is observed to be almost purely so.

According to operator 2 the energy separation between the $^3E'$ and $^3E''$ pair states is equal to $-{}^2/_3(J_{11} - J_{12})$. The ground-state exchange parameter can be expressed in terms of the orbital parameters $J_{ai\,bj}$ as

$$J = {}^1/_9 \sum_{ij} J_{ai\,bj} \tag{5}$$

With relations 4 this reduces to

$$J = {}^1/_3(J_{11} + 2J_{12}) \tag{6}$$

Assuming the orbital parameters $J_{ai\,bj}$ to be the same in the ground and singly excited ^2E pair state, we have the two equalities

$$\begin{aligned} -2J = -{}^2/_3(J_{11} + 2J_{12}) &= 187\ cm^{-1} \\ -{}^2/_3(J_{11} - J_{12}) &= 65\ cm^{-1} \end{aligned} \tag{7}$$

and the corresponding values of the orbital parameters are

$$2J_{11} = -320\ cm^{-1} \qquad 2J_{12} = -125\ cm^{-1} \tag{8}$$

A rationalization of these values is perhaps easier if we make a transformation to a symmetry-adapted basis of one-electron orbitals. The t_2 orbitals transform as a_1 and e in the local C_{3v} point symmetry, and we obtain the following relations of orbital exchange parameters:

$$J_{a_1a_1} = J_{11} + 2J_{12} \qquad J_{ee} = J_{11} - J_{12} \tag{9}$$

With the values in eq 8 the parameters in the symmetry-adapted basis are evaluated as

$$2J_{a_1a_1} = -570\ cm^{-1} \qquad 2J_{ee} = -195\ cm^{-1} \tag{10}$$

Using simple arguments of overlap of magnetic orbitals, we expect $J_{a_1a_1}$ to be the leading antiferromagnetic term. The two a_1 orbitals point directly toward each other, which offers the possibility of a large one-electron transfer integral and thus a large antiferromagnetic $J_{a_1a_1}$. This is supported by the experimental results. The orbital parameters $J_{ai\,bj}$ are often found to be somewhat higher in excited pair states than in the ground state. This would alter the above numbers, but our principal conclusions would not be affected.

It is interesting to compare our results with those obtained for the related dimer systems $Cs_3Cr_2Cl_9$[10] and $Cs_3Cr_2Br_9$.[11] The ground-state *J* parameter is 1 order of magnitude larger in $V_2Cl_9^{5-}$ than in the chromium(III) dimers: $2J = -187\ cm^{-1}$ vs. −13 and −8 cm^{-1}, respectively. The corresponding metal–metal distances are 3.09,[4] 3.12,[11] and 3.30 Å,[12] respectively. The magnetic orbitals are much more contracted in the chromium(III) dimers as a result of the higher nuclear charge. Our analysis of the singly excited pair state is in good agreement with the conclusions reported by Briat et al.[10] on $Cs_3Cr_2Cl_9$. As in our dimer the ratio $J_{a_1a_1}/J_{ee}$ was found to

(9) Geiser, U.; Güdel, H. U. *Inorg. Chem.* **1981**, *20*, 3013.

(10) Briat, B.; Russel, M. F.; Rivoal, J. C.; Chapelle, J. P.; Kahn, O. *Mol. Phys.* **1977**, *34*, 1357.

(11) Wessel, G. J.; Ijdo, D. J. W. *Acta Crystallogr.* **1957**, *10*, 466.

(12) Saillant, R.; Jackson, R. B.; Steib, W. E.; Folting, K.; Wentworth, R. A. D. *Inorg. Chem.* **1971**, *10*, 1453.

be approximately 3. This ratio was rationalized by an extended Hückel calculation.

3. $^2T_1$ and $^2T_2$ Single Excitations. The $^2T_1$ and $^2T_2$ single-ion states are split by the trigonal crystal field. As a result of the large trigonal field the expected splittings are on the order of 500–900 cm^{-1}, with the orbitally nondegenerate component at lower energy in both cases.

Bands f and g in Figure 2 as well as the hot band h can therefore be assigned to the $^2T_{1a0}$ component and the bands above 12 400 cm^{-1} to the $^2T_{1a\pm}$ component. In the $^2T_2$ region bands o and p belong to $^2T_{2x0}$ and the bands q and r to $^2T_{2x\pm}$.

Spin–orbit and exchange coupling produce further splittings. Only one cold transition is allowed to the $^2T_{1a0}$ pair states.[8] It is tempting to assign band f at 12 010 cm^{-1} to this $^1A_1' \rightarrow {}^3A_1'$ transition. It is expected to be σ polarized as observed. Band g does not belong to the pair spectrum, and the hot band at 12 241 cm^{-1} could correspond to the allowed transition $^3A_2'' \rightarrow {}^5A_1'$. This assignment corresponds to a $2J$ value for the $^2T_{1a0}$ singly excited state of approximately −200 cm^{-1}. This is very reasonable in comparison with $2J = -187$ cm^{-1} in the ground state. In the region of $^2T_{1a\pm}$ and $^2T_2$ pair transitions assignments are even riskier and will not be attempted here.

4. ^2E, $^2T_1$ Double Excitations. There are two prominent and sharp bands in the cold absorption spectra of Figure 1, one at 23 888 cm^{-1} in predominant σ polarization and one at 24 625 cm^{-1} in complete π polarization. Their energies correspond approximately to the following sums of single excitations: $^2E + {}^2E$, $^2E + {}^2T_1$. If the energetic effects of the exchange coupling are neglected, double excitations are expected at these energies, and we can confidently assign the sharp absorption bands to these double excitations.

The exchange splitting in the $^2E^2E$ states can be described by operator 2, which was used for the treatment of the single excitations. With $S_a' = S_b' = {}^1/_2$ the possible S' values in the doubly excited states are 0 and 1. $^1A_1' \rightarrow {}^1E'$ is the only spin- and symmetry-allowed transition from the ground pair level to $^2E^2E$. It is expected to be σ polarized, and we assign the 23 880-cm^{-1} band to this transition. The corresponding triplet transition $^3A_2'' \rightarrow {}^3E''$ is expected to lie at approximately the same energy. The temperature dependence of the 23 880-cm^{-1} band does not follow the Boltzmann population expected for a transition originating in $^1A_1'$. Contributions from the hot $^3A_2'' \rightarrow {}^3E''$ transition at higher temperatures are the likely reason for this deviation. The π-polarized 24 625-cm^{-1} band is assigned to the $^1A_2''$ component of $^2E^2T_{1a\pm}$. It can be shown that this is the only allowed transition in π polarization with an exchange intensity mechanism. Energetically this fits nicely: the energies of ^2E and $^2T_{1a\pm}$ single excitations add up to approximately 24 700 cm^{-1}.

5. Conclusions

The spectroscopic study of crystals with the composition $CsMg_{1-x}V_xCl_3$ allows a detailed investigation of the $V_2Cl_9^{5-}$ dimers. The ground-state exchange parameter is determined very accurately by the spectroscopic technique. Transitions to the singly excited ^2E pair states can be studied in detail. Due to their sharpness they allow the measurement of Zeeman absorption spectra, which are of great value for the characterization of the excited pair states. The analysis of the energetic splitting of the ^2E state allows the determination of orbital exchange parameters $J_{ai\,bj}$ contributing to the total J and thus provides some information on the dominant exchange pathways. Such information is not available from a study of the ground-state properties alone.

Acknowledgment. We are indebted to A. Hauser for preliminary synthetic and spectroscopic work and numerous fruitful discussions. Financial support by the Swiss National Science Foundation (Grant No. 2.427-0.79) is gratefully acknowledged.